www.cat-science.cat

Nanomechanics of Langmuir-Blodgett films

Juan Torrent-Burgués[1]*, Gerard Oncins[2], Fausto Sanz[2]

1. Departament d'Enginyeria Química, Universitat Politècnica de Catalunya

2. Departament de Química Física, Universitat de Barcelona i Institut de Bioenginyeria de Catalunya

Resum

La caracterització topogràfica i nanomecànica de pel·lícules moleculars és important degut al creixent interès que aquestes desperten, tant des del punt de vista científic com tecnològic. Com a cas particular tenim les pel·lícules Langmuir i Langmuir-Blodgett (LB), les quals permeten el control de l'àrea per molècula i per tant de la nanoestructura de la mostra. Les pel·lícules Langmuir poden caracteritzar-se en la interfase aire-aigua mitjançant les isotermes de pressió superficial-àrea i amb el Microscopi d'Angle de Brewster (BAM). Les mesures de pressió superficial proporcionen informació global de la pel·lícula mentre que el BAM proporciona imatges òptiques d'àrees de dimensions mil·limètriques amb resolució lateral a escala micromètrica. Les pel·lícules Langmuir poden ser transferides a un substrat pla (pel·lícules LB) i poden estudiar-se a escala nanomètrica mitjançant les Microscopies de Sonda Local (SPMs). Entre elles, la Microscòpia de Forces Atòmiques proporciona imatges topogràfiques, mentre que la Microscòpia de Forces Laterals i l'Espectroscòpia de Forces proporcionen informació sobre les propietats nanotribològiques i nanomecàniques de les pel·lícules. En aplicar aquestes tècniques a l'estudi de pel·lícules mixtes, proporcionen informació sobre miscibilitat, separació de fases, estructura de dominis i propietats mecàniques. Degut a la possibilitat de controlar la pressió superficial de la pel·lícula, es pot correlacionar aquest valor amb l'estructura i el comportament nanomecànic de les capes.

Paraules clau: monocapa Langmuir · pel·lícula Langmuir-blodgett · microscòpia de força atómica · microscòpia de força lateral · espectroscòpia de forces · microscòpia d'angle de Brewster · isoterma pressió superficial-àrea

Abstract

The topographical and nanomechanical characterization of molecular films is an important issue due to the increasing interest in this kind of 2-dimensional structure, both from a scientific and technological point of view. In particular, Langmuir and Langmuir-Blodgett (LB) films have been widely studied as it is possible to control the area per molecule in the layer, with the consequent control over the sample nanostructure. Langmuir films can be characterized at the air-water interphase by using surface pressure-area isotherms and Brewster Angle Microscopy (BAM). Surface pressure measurements provide information on the films as a whole and BAM provides optical images of areas in the millimetric range with lateral resolution on the micrometric scale. Langmuir films can be transferred onto an atomically flat substrate and the transferred films (LB films) can be studied in the nanometric range using Scanning Probe Microscopies (SPMs). Of these, Atomic Force Microscopy provides topographical information, while Lateral Force Microscopy and Force Spectroscopy provide information about the nanotribological and nanomechanical properties of the films. These techniques, when applied to the study of mixed films, provide information about miscibility, phase separation, domain structure and mechanical properties. In this respect, SPMs can provide information at a nanometric level that it is not available using BAM. Thanks to the possibility of controlling the film surface pressure, correlation between sample nanostructure and nanomechanics can be established.

Keywords: Langmuir monolayer · Langmuir-Blodgett film · atomic force microscopy · lateral force microscopy · force spectroscopy · Brewster angle microscopy · surface pressure-area isotherm

1. Introduction

Langmuir and Langmuir-Blodgett (LB) films are organized nanometric systems of scientific and technological interest, and since the development of the technique in 1935 [1] a wide range of monolayers and multilayers of different molecules have been studied [2-5], being a matter of extensive research

* Author for correspondence: Juan Torrent-Burgués. Departament d'Enginyeria Química, Universitat Politècnica de Catalunya. Colom 1. 08222 Terrassa, Barcelona, Catalonia, EU. Tel. +34 937398043. Fax +34 937398225. Email: juan.torrent@upc.edu

in recent years because of their suitability as models for the study of molecular organization [6-15]. The possibility of controlling the chemistry of the subphase, the area per molecule and the extraction surface pressure of the layers is a potentiality of this technique, which has been widely used to prepare all kinds of ordered structures as varied as phospholipid bilayers [16], nanowire arrays [17] and surfaces with tailored chemical, structural and mechanical properties. This, as well as the emergence of Micro- and NanoElectromechanical systems (MEMS and NEMS) and the consequent necessity to produce lubricants at a molecular level, have led to the extensive use of LB films to obtain low-friction coatings for the electronics industry [18, 19]. In this scenario, fatty acid LB films have become useful model systems because of their linear geometry, amphiphilic nature and high mechanical stability and durability. From an applied point of view, LB films are used in molecular electronics, optics and also in sensor development, the latter field being the one where macrocyclic compounds such as crown ethers have demonstrated outstanding performance, especially acting as metal ionophores. Due to all of this, the formation of LB films with this kind of compound [20-22] is interesting because of their obvious sensing applications but also because of the whole structural, nanomechanical and functional information that can be obtained by combining Atomic Force Microscopy (AFM) and the LB deposition technique.

Scanning Probe Microscopies (SPMs) have been proven to be suitable for the study of monolayers or bilayers at a molecular level [23, 24] from a topographical, electrical, magnetic and mechanical point of view. In this sense, AFM has become the most used SPM technique to study LB films [2, 3, 13, 25], mainly as a topographic tool. Lateral Force Microscopy (LFM) has become an increasingly popular technique for the study of the nanotribological properties of surfaces and supported films [26-33]. This has partly been promoted by the development of suitable techniques to calibrate the vertical [34-38] and lateral [39, 40] spring constants of the probes used in LFM measurements, allowing quantitative friction results in the NanoNewton range to be obtained [27-29]. In particular, LFM has been used to study the frictional properties of several Langmuir-Blodgett layers [41-43].

The molecular structure of fatty acid LB films has been studied by several authors [44-49]. A recent work concluded that the nanomechanical properties of arachidic acid (AA), behenic acid (BA) and stearic acid (SA) strongly depended on the film extraction pressure [49]. In this direction, the study of the dependence between monolayer thickness and the vertical force applied by the tip on several fatty acid monolayers (F_v), showed that there is an initial decrease in thickness attributed to the creation of gauche defects in the alkyl chain terminal ends at low F_v values, followed by a constant thickness regime and by a final monolayer rupture after a threshold F_v value is reached [49]. A similar study performed on BA [50, 51] indicated that the monolayer thickness evolution vs. F_v also depended on the monolayer phase; different monolayer phases respond with different friction force (F_f) vs. F_v trends, showing that the F_f value is highly sensitive to the monolayer molecular ordering. Another important factor concerning the mechanical properties of LB monolayers is the length of the alkyl chain, which modifies the intermolecular van der Waals interactions. So, the longer the chain, the higher the F_v value at which the monolayer breaks during scanning [49]. Van der Waals interactions and, consequently, the frictional response can also be modified by varying the monolayer extraction pressure [52].

Mixed films are highly interesting systems, as they are present in natural systems such as biomembranes. Mixed films have been widely studied to investigate their phase separation, especially in those systems with notable applied interest, such as phospholipids or fatty acids. In these mixtures the components are structurally similar but differ in terms of chain length, head group or halogen substitution. The effect of these parameters on the mixing behaviour has been reported [53-65] and it has been concluded that significant differences in these parameters lead to phase separation. Systems with structurally dissimilar components have also been investigated [66-81]. AFM in the topographic mode has become a common technique in the study of mixed LB films, but related techniques such as Force Spectroscopy (FS) or LFM [53, 56, 69, 82-84] have been less used. These techniques provide quantitative and extremely local mechanical information, so variations in response between different zones of the film due to different chemical composition or differences in structure or molecular orientation can be assessed. The formation of separated phases is an important phenomenon in mixed films and these techniques provide a powerful tool for its investigation, especially when domains present micrometric or nanometric size.

The aim of this work is to present the study of the formation of the Langmuir films of a fatty acid, a macrocyclic compound with sensor properties and their mixtures at the air-water interphase using surface pressure-area isotherms and Brewster angle microscopy (BAM), as well as the morphological and mechanical study of the deposited LB films using AFM, LFM and FS. The correlation between the surface pressure-area isotherms and the measured F_f values obtained by LFM on the monolayers gives useful nanotribological information and the F_f vs. F_v curves provide information about the different frictional stages that range from non-contact between the sample and the AFM probe to the total disruption of the monolayer. The nanomechanical properties of these monolayers under vertical compression are tested as a function of the extraction pressure by means of FS.

2. Techniques

2.1. Surface pressure-area isotherms. LB film formation

The studied compounds were dissolved in chloroform and spread onto the aqueous subphase, which was pure water Millipore MilliQ grade. During the film compression process at the air-water interphase (Figure 1*a-b*), the surface pressure (Π) is recorded against the area (surface pressure-area isotherm), which gives us information about the film states, phases and phase transitions. Π is the difference between the surface tension of pure water (γ_o) and that of the film (γ), that is, $\Pi = \gamma_o - \gamma$. Surface pressure-area isotherms were obtained in a NIMA

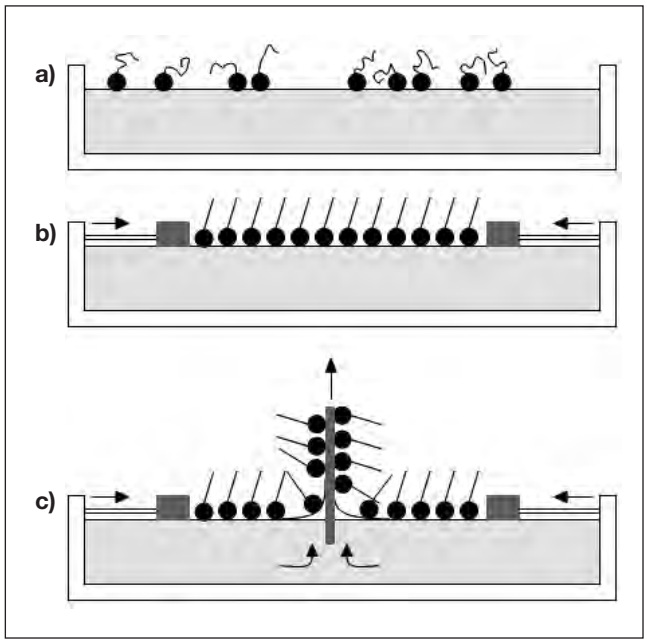

Figure 1. Formation of a fatty acid LB film. a) Molecules accumulate on the water surface with the hydrophilic groups towards the water and the hydrophobic chains towards the air. b) Two barriers compress the molecules while Π is controlled. c) At the desired Π, the mica substrate emerges from the liquid and the fatty acid molecules become stuck to its surface. The barriers compress the remaining monolayer so as to maintain a constant Π value as molecules are removed from the liquid surface.

Langmuir-Blodgett trough placed on an isolation platform and the Π value was measured using the Wilhelmy method with the NIMA trough and using a paper sheet. The isotherms were fairly reproducible. The BAM makes it possible to obtain images of the monolayers at the air-water interphase and the equipment used was a NIMA-Nanofilm microBAM, which uses a 6 mm diameter collimated beam and gives a lateral resolution of 8 μm.

The LB films were transferred at constant Π onto freshly cleaved atomically flat red mica sheets (1 cm × 1 cm) and samples at different Π values were extracted. The transfer process was performed using a NIMA dipper and following a Z deposition (Figure 1c), that is, the sheet of mica is first introduced in the subphase prior to the formation of the monolayer onto the water subphase, and once the Langmuir film is compressed to the desired Π value, the mica sheet is pulled up. The transfer ratio for the LB films, that is the ratio between the decreased film area during the transfer process and the immersed substrate area, was close to 100%.

2.2. AFM, LFM and FS measurements

AFM images were obtained in Nanoscope Multimode equipment (Digital Instruments, CA) using contact and tapping modes. Tapping mode images were obtained using silicon microfabricated cantilevers with a nominal vertical spring constant (k_v) of 40 N/m, while contact mode images were obtained with silicon nitride cantilevers with a nominal k_v value of 0.16 N/m. LFM measurements (see Figure 2) were conducted with a Dimension 3100 microscope attached to a Nanoscope IV controller in contact mode using V-shaped Si_3N_4 tips with nominal k_v values of 0.08 and 0.02 N/m. Force curves were always performed before acquiring topographic images in order to apply the minimum vertical force on the surface so as to avoid any monolayer damage. The instrument was placed on a vibration isolation table and enclosed in an isolation box. Temperature and humidity were controlled during experiments and maintained between 20-22º and 35-50%RH respectively. AFM, LFM and FS measurements on several LB films transferred to the same conditions show good enough reproducibility.

The k_v value of the tips used in LFM and FS experiments was individually and experimentally measured by means of a Force Probe1-D MFP AFM (Asylum Research, CA) using the thermal noise method [38]. The lateral spring constant (k_l) of the tips used in LFM experiments was calculated using the wedge calibration method developed by Ogletree et al. [39], and the raw data treatment was performed with Matlab scripts provided by the R. Carpick group [85]. Briefly, the scripts were used to analyze F_f vs. F_v curves that were experimentally obtained using a home-made electronics card to lineally increase the F_v value while simultaneously recording the F_f signal. Further experimental details can be found elsewhere [86].

Triangular Si_3N_4 tips with a nominal k_v value of 0.5 N/m (Microlever Probes model MLCT-AUNM, Veeco, CA) were used in FS measurements, which were performed using the Force Volume routine implemented in the Nanoscope software; basically, it performs a grid of single force curves in a selected area, ensuring that each force curve is done in a fresh spot. In this study, 64x64 force curves per image were acquired with a linear tip velocity of 1-2 μm/s. In addition to the spectroscopic information, the topographic profile was also recorded at each location, so force curves can be unmistakably related with the sample morphology. The data analysis was performed with the AFM Force Volume Data Analysis Software. The sample penetration (P_d) during a force curve was calculated as $P_d = \Delta Z - \Delta x$, being ΔZ the force curve vertical piezo displacement and Δx the cantilever vertical deflection in the contact region.

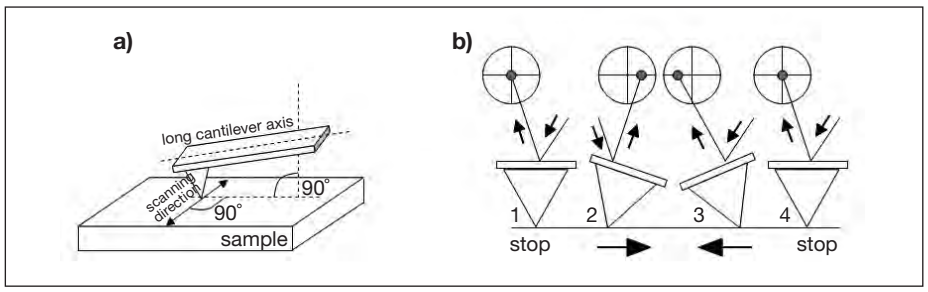

Figure 2. LFM operation. a) The tip scans the surface perpendicularly to the main cantilever axis. b) Whole friction measurement (friction loop): 1 – the cantilever stands still on the surface. 2 – the tip scans the sample from left to right, creating a cantilever torsion that is detected by the photodetector. 3 – the same process but scanning from right to left. Now the laser spot is on the left side of the photodetector. 4 – end of the loop.

3. Results and discussion

3.1. Isotherms at the air-water interphase

Arachidic acid (AA), or eicosanoic acid ($CH_3(CH_2)_{18}COOH$, M = 312.0), is a fatty acid with the typical amphiphilic structure suitable for Langmuir film formation at the air-water interphase; the hydrophilic head (carboxylic acid group) orients towards the water subphase while the hydrophobic hydrocarbon chain points to the air. Figure 3 shows the surface pressure-area per molecule isotherm for a film of AA together with BAM images captured at several points of the isotherm. The AA film isotherm presents several states or phases during compression; the first one corresponds to the raising zone comprised between 0 and 25 mN/m and is characterized by a compressibility coefficient (β) of ca. 9.0 10^{-3} m/mN (β^{-1} = 110 mN/m), which corresponds to a liquid condensed phase, while the second raising zone (from 25 to 56 mN/m) presents a β value of ca. 2.6 10^{-3} m/mN (β^{-1} = 380 mN/m) corresponding to a solid phase. BAM images clearly show that the film becomes more compact and uniform as the compression increases. Finally, when the surface pressure reaches a value ca. 56 mN/m, the film collapses.

Figure 4 shows the surface pressure-area isotherm corresponding to a film of a copper(II) ionophore macrocyclic compound (MC) that is potentially interesting for sensing applications, 4-phenyl-4-sulfide-11-(1-oxodecyl)-1,7-dithia-11-aza-4-phosphacyclotetradecane, M = 513.8, with the corresponding BAM images at several points in the isotherm. The raising part of the isotherm presents a β value of ca. 25 10^{-3} m/mN and corresponds to a liquid expanded state which appears as a uniform film in the BAM image. After reaching a surface pressure ca. 12-13 mN/m the isotherm forms a quasi-plateau reaching areas per molecule much lower than the molecular area, indicating that a multilayer is formed at this stage. The BAM images show the presence of a granular structure that corresponds to the multilayer formation, although further structural information cannot be obtained as the size of the structures is lower than the BAM resolution limit.

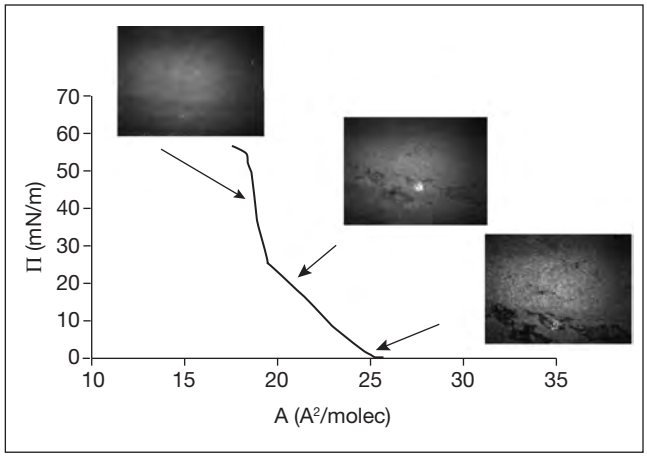

Figure 3. Surface pressure-area isotherm and BAM images, at several locations in the isotherm, for an AA monolayer.

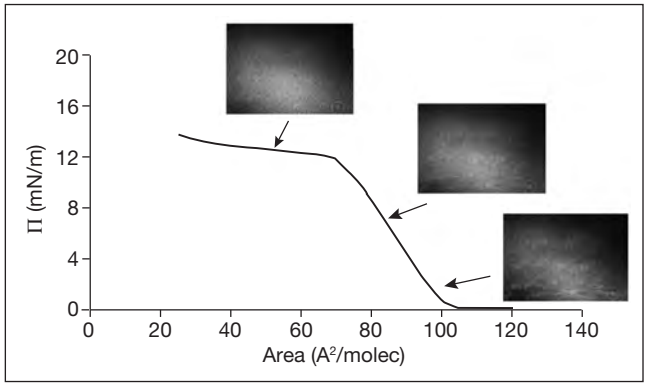

Figure 4. Surface pressure-area isotherm and BAM images, at several locations in the isotherm, for a MC film.

Figure 5 shows the surface pressure-area isotherm for a mixed film of AA and MC at the composition of C_{AA}/C_{MC} = 1/2 (C_{AA} = 0.333 mg/mL, C_{MC} = 0.666 mg/mL; X_{MC} = 0.55), where the X axis represents the area referred to the MC molecules, that is, the total area divided by the number of MC molecules. The shape of this isotherm resembles the combination of the individual isotherms of AA and MC. BAM images show a uniform film for Π values up to the first raising zone and a non-uniform film at the plateau, corresponding to the formation of an MC multilayer that is not prevented by the presence of AA molecules.

Figure 6 represents the excess area (A_{ex}) vs. composition for several mixed films of AA and MC. A_{ex} is defined by equation 1, where A_i and x_i are the areas in the individual isotherms and the molar fractions in the mixture, respectively. If the additivity rule is fulfilled, then A_{ex} = 0, indicating an ideal mixture or immiscibility. The analysis of the performed experiments for mixed films of AA-MC show a positive value for A_{ex}, which indicates a certain degree of miscibility and that interactions between AA and MC molecules are less favourable than those corresponding to pure substances.

$$A_{ex} = A_{exp} - A_{ad} = A_{exp} - (x_1A_1 + x_2A_2) \quad (1)$$

For a given composition, the A_{ex} value decreases when the Π value increases, indicating that the alkyl chains adopt a more perpendicular orientation with respect to the substrate, favouring a better interaction between AA and MC molecules. β values calculated in the first raising zone of the isotherms for the mixed monolayers are more similar to those obtained for pure MC monolayers but change according to the composition. It is possible to make a similar analysis to that performed for A_{ex} but now with β. Using the definition of β, equation (2), and applying equation (1), the following additivity rule (equation 3) is obtained for ideal mixing or immiscibility:

$$\beta = \frac{1}{A}\left(\frac{\partial A}{\partial \Pi}\right) \quad (2)$$

$$\beta_{ad} = \frac{1}{A_{ad}}\left(\frac{\partial A_{ad}}{\partial \Pi}\right) = \frac{\beta_1 x_1 A_1 + \beta_2 x_2 A_2}{x_1 A_1 + x_2 A_2} \quad (3)$$

where β_i is the compressibility coefficient in the film of pure component *i* at a given Π value. From the β_{ad} values calculated with equation (3) and those obtained experimentally with equation (2), it is observed that the additivity rule is not fulfilled, with experimental β values slightly higher than those calculated with equation (3).

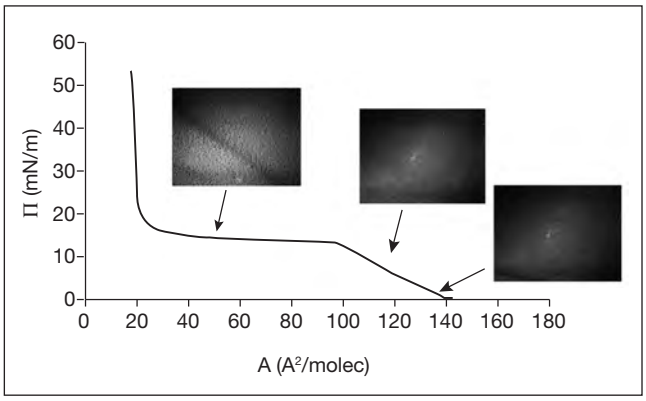

Figure 5. Surface pressure-area isotherm and BAM images, at several locations in the isotherm, for an AA-MC (1:2) mixed film. The area refers to the MC molecules.

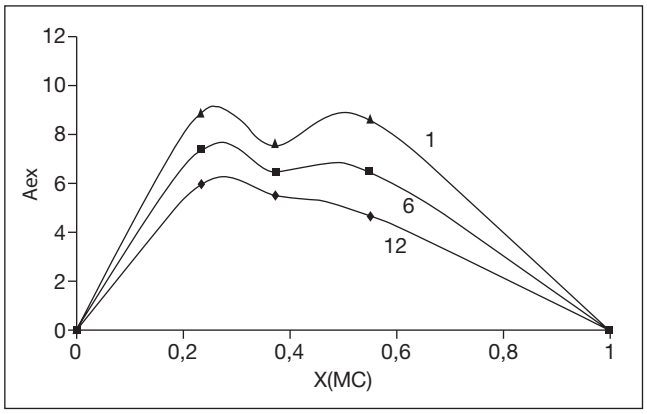

Figure 6. Excess area vs. Composition for mixed films of AA-MC at Π = 1 (Δ), 6 (□), 12 (◇) mN/m.

3.2. AFM and related techniques (LFM, FS)

Figure 7 shows AFM images of AA LB monolayers extracted at different Π values and the monolayer height vs. Π value. Samples extracted at 15 mN/m (liquid condensed) and 35 mN/m (solid) show domains of different thickness corresponding to different tilting angle orientations of the AA molecules in the monolayer. As the Π value increases, the molecules orient more vertically with respect to the substrate and the tilting angle, considered the angle formed between the molecules and the perpendicular to the substrate, decreases. This change of orientation results in a higher molecular ordering, as the molecules are forced to pack more tightly and, therefore, to maximize intermolecular interactions. The nanometric or submicrometric size of the different tilted domains is below the BAM resolution and can only be observed using SPM techniques. The effect of domain thickness discretization was observed in the past by several authors [87-89] for alkanesilanes and alkanethiols monolayers and attributed to the interlocking between the hydrocarbon chains of the molecules. Then, as the zigzag structure of the chains only allows certain angles that maximize van der Waals interactions, the thickness of the cited monolayers changes in discrete steps.

The nanomechanical properties of the monolayer depends on the AA molecular orientation, and consequently on the Π value. Table 1 presents the F_v values needed to break the monolayer (breakthrough force) vs. Π value. These breakthrough forces were calculated using two different techniques. Firstly, force curves were performed on the samples and the monolayer breakthrough was detected as a small discontinuity in the contact region of the curve [90]. Secondly, LFM was applied to obtain F_f vs. F_v curves, which enclose the nanotribological information of the monolayers since an increasing pressure is applied to them until they are completely disrupted. Then, the ongoing of sample rupture is detected as a steep increment in the F_f value. It is important to note that crossover between topographic and lateral signals can be significant during the performance of friction measurements. Nevertheless, in the case of monolayers, topographic signal is low enough to consider the crossover insignificant and negligible in the interpretation of LFM results. To begin with, the breakthrough forces attained by FS and LFM experiments increase with the sample extraction Π value, so it is clear that the nanomechanical response of the monolayers depends on the sample structure and on the intermolecular distance. Obviously, when the Π value increases the molecules are packed more tightly, the intermolecular interactions grow stronger and the structure is more difficult to puncture. Interestingly, the breakthrough F_v values obtained by FS and LFM experiments, despite showing the same trend with the Π value, are noticeably different. This is due to the different nanomechanical nature of the experiments performed; while FS tests the response of the monolayer as a pure vertical compression is performed, LFM gathers the response of the sample while the tip scans the surface at an increasing F_v value.

Table 1. Arachidic acid LB film breakthrough forces for different extraction *P* values.

Breakthrough force (nN)	*From force curves*	*From F_f vs. F_v curves*
Π = 1 mN/m	13.1 ± 3.2	6 ± 2.1
Π = 15 mN/m	15.3 ± 4.9	12 ± 3.5
Π = 35 mN/m	22.9 ± 5.5	15 ± 3.0

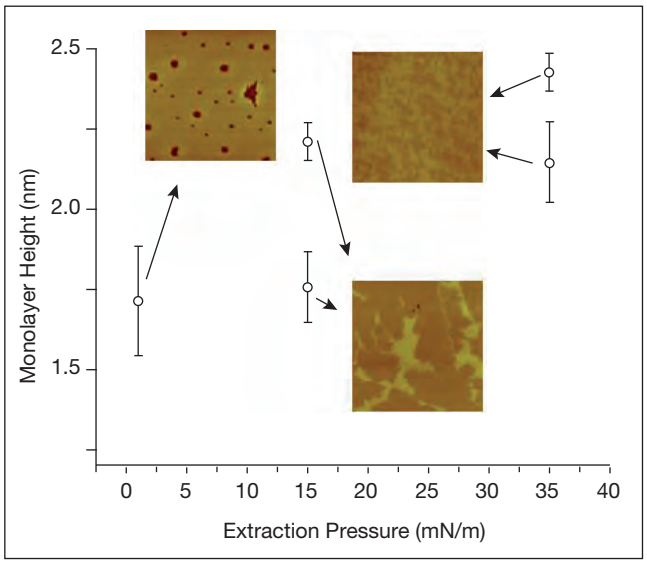

Figure 7. AFM images (5x5 μm²) of LB films of AA at Π values of 1, 15 and 35 mN/m and the corresponding measured heights.

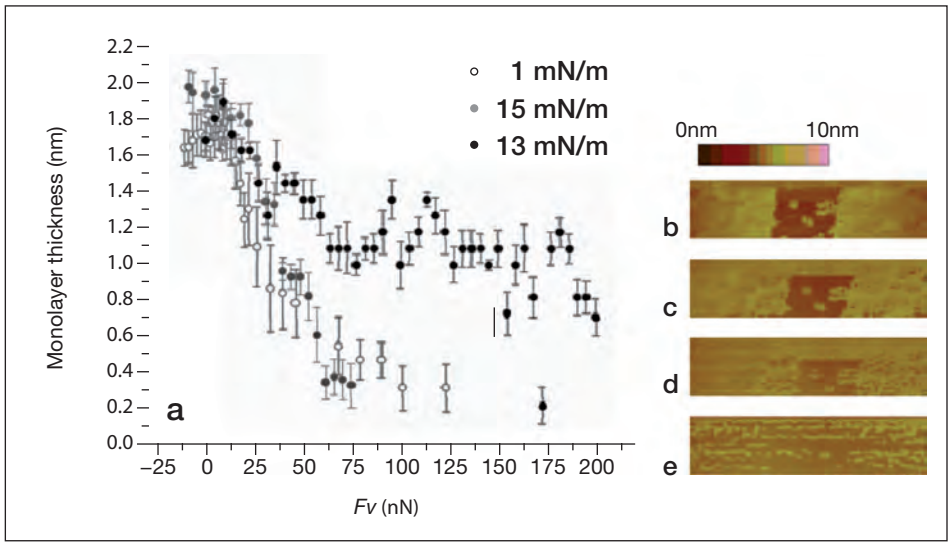

Figure 8. Wear experiments performed on AA monolayers extracted at different Π values. a) The monolayer thickness is depicted as a function of the F_v applied to the sample. AFM topographic images (5μm x 1.5μm) of the sample surface obtained at different F_v values: b) 0 nN; c) 27 nN; d) 73 nN; e) 145 nN.

Figure 8 shows wear experiments on an AA monolayer extracted at 35mN/m. Basically, this kind of experiments consists of capturing series of topographic images of a certain region at an increasing F_v value so as to assess the morphological changes that the monolayer undergoes. In order to measure the monolayer thickness, a patch of monolayer is removed prior to the experiment by applying an F_v value ca. 300 nN to the central region of the area of study (central region in Figures 8*b* to *e*). As can be seen in Figure 8*a* the AA monolayer thickness decreases as the F_v value increases, independently of the extraction Π value. It also is interesting to note that the decrease in monolayer thickness is not linear but stepped, in concordance with the hydrocarbon chain interlocking model presented before. In addition, it is noteworthy that the deformation rate decreases when the extraction Π value increases, as would be expected because of the higher layer compactness and intermolecular interaction.

Figure 9 shows the topographic and friction images of MC monolayers extracted at several Π values. On the one hand, it is seen that MC molecules form a practically homogeneous monolayer where small island-like domains can be seen, the height of which increases with the Π value. The size of these domains is lower than the lateral resolution of BAM and for this reason optical images appear uniform and homogeneous. Considering the nanomechanical response of the samples, the island-like domains present a higher friction signal than the surroundings, indicating that MC molecules are probably less ordered in these domains [91]. Another interesting observation is that domains which are not seen in the topographic image sometimes appear in the friction one (Figure 9*b*) and that these domains even present a higher friction signal, indicating that we are dealing with more disordered domains in the MC monolayer. The friction loops recorded in the forward and reverse scan (see Figure 2), and obtained at the island domains, show that they depend on the extraction Π value. Then, symmetric friction loops are obtained at Π = 4 mN/m while the ones obtained at Π = 12 mN/m are asymmetric. At Π = 8 mN/m, the higher domains show asymmetric friction loops, while the lower ones show symmetric friction loops. This friction behaviour is related with the domain formation process, with domains in process of formation showing symmetric friction and already formed domains showing asymmetric friction.

Figure 10*a* shows F_f vs. F_v curves performed on three LB films of compound MC deposited on mica at Π values of 4, 8 and 12 mN/m. The jump in the F_f signal indicates the monolayer rupture and the corresponding F_v necessary to break the films are represented in Figure 10*b*. Again, these experiments demonstrate that there is a direct dependence between the Π value and monolayer mechanical resistance.

AFM topographic images of mixed films of AA-MC, with compositions C_{AA}/C_{MC} = 2/1 (2:1) and C_{AA}/C_{MC} = 1/2 (1:2), are shown in Figure 11. From direct observation, large island-like domains (type I) embedded in a continuum monolayer can be seen. Also, in Figure 11*a* two small islands of a different nature (type II) can be seen in addition to the type I central domain.

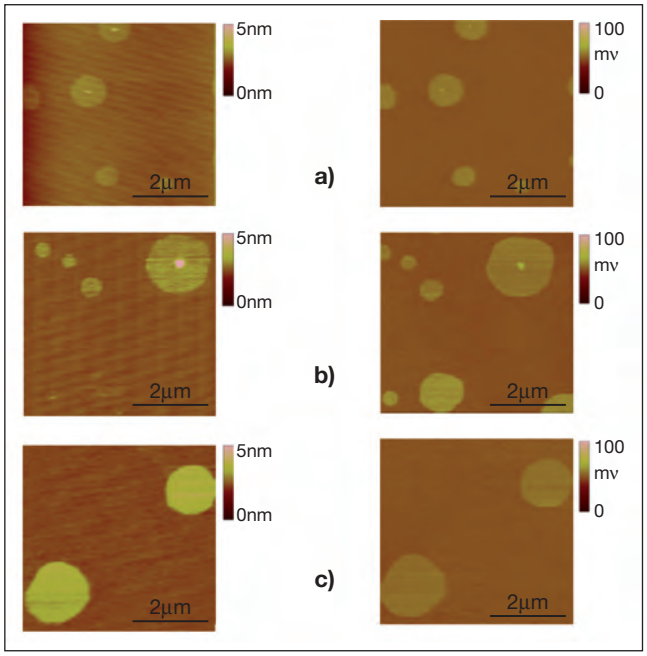

Figure 9. Topographic (left) and friction (right) images of MC LB films extracted at: a) Π = 4 mN/m, b) Π = 8 mN/m, c) Π = 12 mN/m.

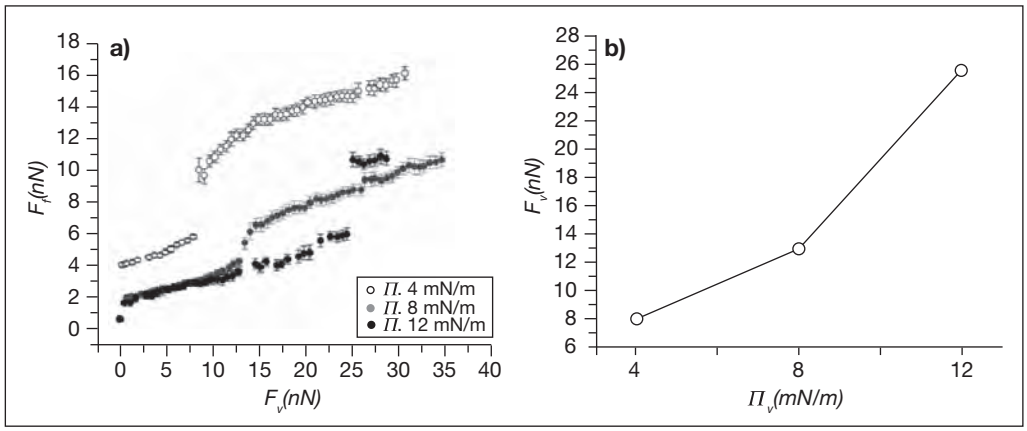

Figure 10. a) F_f vs. F_v curves performed on MC monolayers extracted at 4, 8 and 12 mN/m. b) F_v values at which the MC monolayers break when performing the F_f vs. F_v curves (the monolayer rupture can be detected as a sudden increment in the F_f signal in Fig. 10*a*).

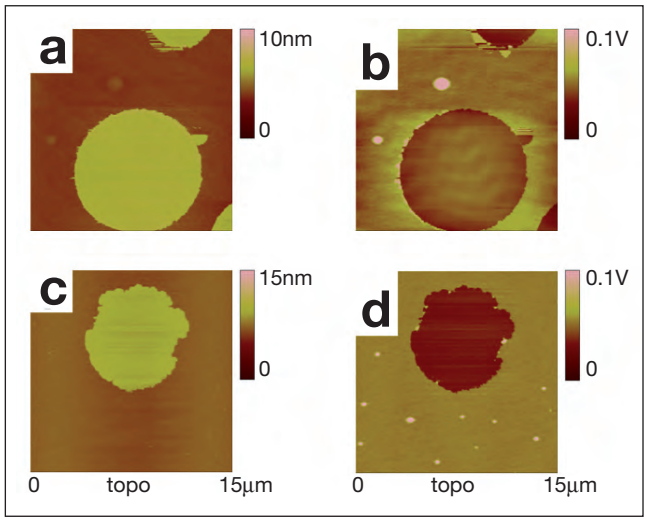

Figure 11. 15µm x 15µm AFM topographic (a, c) and frictional (b, d) images obtained on an AA/MC (2:1) (a, b) and an AA/MC (1:2) (c, d) mixed monolayer extracted at Π = 10 mN/m and supported on mica.

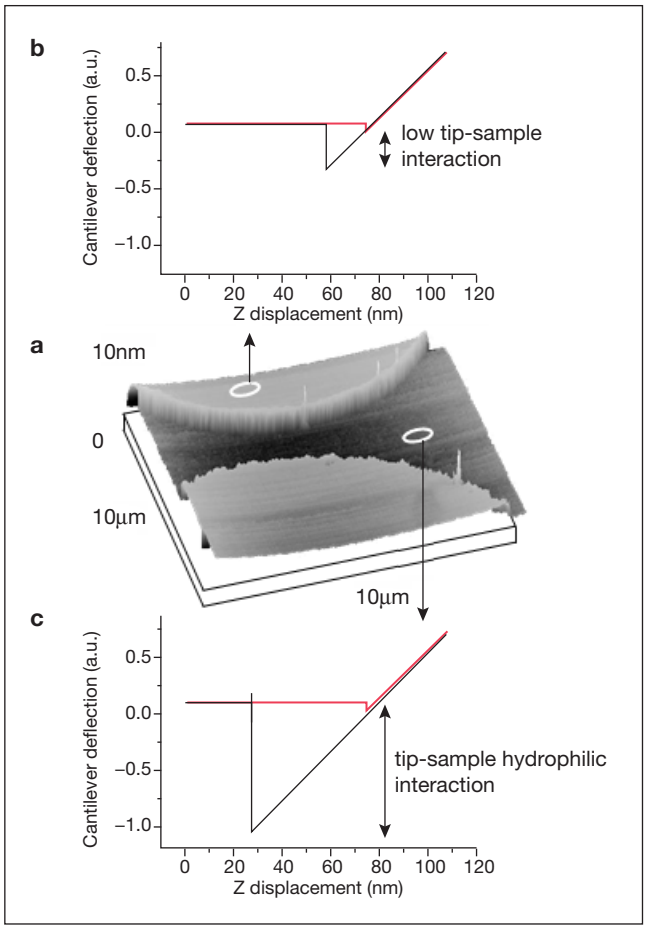

Figure 12. Quantification of adhesive forces between the AFM tip and the different phases of an AA/MC mixed monolayer. a) 10µm x 10µm AFM topographic image. Force curves were acquired on type I domains (AA phase, Fig. 12*b*) and on the MC phase (Fig. 12*c*).

They are barely visible in the topographic image as their thickness is very similar to that of the surrounding continuum monolayer. Nevertheless, they can easily be detected in the friction image presented in Figure 11*b* where it is also seen that the type I domains present a lower friction signal than the continuum monolayer and that the type II islands display the highest friction response. The same phenomenon can be observed in Figures 11*c* and *d*. Another fact observed after the analysis of several topographic images performed on different spots of the sample and on different samples is that the area percentage occupied by type I island-like domains increases when the ratio of AA increases in the mixture. These facts suggest that type I domains are AA domains while the surrounding continuum monolayer is the MC phase. Also, the height of type I domains is in close agreement with the height of the AA molecules when disposed vertically. Friction signal also renders interesting information when it comes to elucidate the composition of the different phases present in a monolayer; as said before, type I domains present the lower friction as it would correspond to the interaction between the hydrocarbon hydrophobic chains of the fatty acid and the hydrophilic AFM tip. On the other hand, the continuum phase presents a higher friction signal because the MC, despite having a hydrocarbon chain, is also formed by hydrophilic moieties. Finally, and regarding type II domains, we believe that they are also MC domains but in a disordered state which would corroborate the high friction response they display.

Figure 12 presents another different nanomechanical behaviour that can be extracted from FS experiments. During a force curve, the AFM tip indents the sample surface and after that, it returns to the initial rest position. During the retraction process, adhesive forces arise between the tip and the sample that can be detected as a cantilever deflection and transformed into

quantitative F_v values. In the case of mixed AA/MC monolayers, adhesion measurements are highly instructive for understanding the different interactions between tip and sample; Figure 12*a* presents a 3D topographic image of the mixture where type I domains and MC phase can be seen. Force curves performed on the type I domains (Figure 12*b*) show a low adhesive force between the two surfaces; considering that the presented measurements were performed in an air environment we should consider that ambient water plays a key role in adhesive phenomena. Then, as type I domains are AA and the hydrocarbon chains of AA molecules point towards the air interface, there is no water on the top of the domains, so the tip (hydrophilic) does not interact and adhesion is low. On the other hand, the MC phase (Figure 12*c*) has hydrophilic groups that favourably interact with water, resulting in a strong interaction with the tip.

4. Conclusions

The Langmuir-Blodgett deposition technique makes it possible to obtain organized molecular films with an accurate control of the area per molecule and the surface pressure, which are factors that strongly influence the topographical and nanomechanical characteristics of the films. Atomic Force Microscopy provides topographical information with a lateral resolution in the range of tens of nanometers and allows us to observe structural details which could not be seen by means of Brewster Angle Microscopy. Lateral Force Microscopy and Force Spectroscopy provide information on the nanotribological and nanomechanical properties of the films while the formation of domains corresponding to different tilting angle orientation phases in arachidic acid films has been observed by topographic Atomic Force Microscopy. In this sense, as the monolayer surface pressure increases, arachidic acid molecules orient more perpendicularly to the substrate, and the vertical force values needed to break the film become higher. Domain formation has also been observed in films of a macrocyclic compound and these domains present a higher friction signal than the surrounding monolayer. We have stated that, as surface pressure increases, the height of these domains increases; and the force needed to break the monolayer also increases. When the study was performed on mixed films of arachidic acid and the macrocyclic compound, information about miscibility and phase separation was obtained. A domain structure is observed in the mixed films and the measurement of the topography and the mechanical properties enable us to identify them. Concerning the sample morphology, three different phases were detected; first of all, an arachidic acid phase forming large island-like domains, surrounded by a continuum macrocycle phase; these arachidic acid domains present a lower friction signal and lower adhesion forces than the surrounding macrocycle phase. The third is a disordered macrocycle phase that presents small island-like domains; these domains, despite showing the same thickness as the surrounding macrocycle phase and being barely distinguishable by means of topographic images, present a noticeable friction contrast because of their distinctive nanostructure.

We can conclude that the study of the nanotribological and nanomechanical properties of Langmuir-Blodgett films makes it possible to resolve interesting nanostructural aspects, both in pure and mixed films.

Acknowledgements

This work was supported by the Generalitat de Catalunya through project PIR2002-00167, and by MCYT through project CTQ2007-68101-C02. Thanks to M. Pla and A. Errachid for providing the compound MC.

References

[1] a) Blodgett K.B. (1934). *J. Am. Chem. Soc*. 56:495, b) Blodgett K.B. (1935). *J. Am. Chem. Soc.* 57:1007, c) Blodgett K.B., Langmuir I. (1937). *Phys. Rev.* 51:964

[2] Ulman A. *"An Introduction to Ultrathin Organic Films"*. Academic Press, Boston, 1990.

[3] Petty M.C. (1996). *Langmuir-Blodgett Films: An Introduction*, Cambridge University Press, Cambridge, ch. 3.

[4] Richardson T.H., in Functional Organic and Polymeric Materials, T.H. Richardson Editor, John Wiley and Sons, Ltd, Chichester, 2002, ch.5.

[5] Stine K.J., Moore B.G. Nano-Surface Chemistry, M. Rosoff Editor, Marcel Dekker, Inc., New York, 2002.

[6] Maheshwari R., Dhathathreyan A. (2004). *J. Colloid Interf. Sci.* 275:270

[7] Cattaneo S., Rouhento C., Vuorimaa E., Efimov A., Lemmetyinen H., Kauranen M. (2003). *Chem. Phys. Lett.* 377:306

[8] Harbottle R.R., Nag K., Intyire N.S., Possmayer F., Petersen N.O. (2003). *Langmuir* 19:3698

[9] Bjornholm T., Hassenkam N. (1999). Reitzel, *J. Mater. Chem.* 9:1975

[10] Hertmanowski R., Martynski T., Bauman D., Mol J. (2005). *Struct.* 741:201

[11] Wohnrath K., Constantino C.J.L, Antunes P.A., dos Santos P.M., A.A.Batista, R.F. Aroca, O.N. Oliveira Jr. (2005). *J. Phys. Chem.* B 109:4959

[12] Huang X., Jiang S., Liu M. (2005). *J. Phys. Chem.* B 109:114

[13] a) Leporatti S., Bringezu F., Brezesinski G., Möhwald H. (1998). *Langmuir* 14:7503; b) Leporatti S., Brezesinski G., Möhwald H. (2000). *Colloids Surf.* A 161:159

[14] Sanyal M.K., Mukhopadhyay M.K., Mukherjee M., Datta A., Basu J.K., Penfold J. (2002). *Phys. Rev.* B 65(3):033409/1

[15] Takamoto D.Y., Aydil E., Zasadzinski J.A., Ivanova A.T., Schwartz D.K., Yang T., Cremer P.S. (2001). *Science* 293:1292

[16] Kiessling V., Crane J.M., Tamm L.K. (2006). *Biophys. J.* 91:3313

[17] Tao A., Kim F., Hess C., Goldberger J., He R.R., Sun Y.G., Xia Y.N., Yang P.D. (2003). *Nano Lett* 3:1229

[18] Cong P., Nanao H., Igari T., Mori S. (2000). *Appl. Surf. Sci.* 167:152
[19] Ren S-L., Yang S-R., Wang J-Q., Liu W-M., Zhao Y-P. (2004). *Chem. Mater.* 16:428
[20] Winter H-J., Manecke G. (1985). *Makromol. Chem.* 186:1979
[21] Badis M., Tomaszkiewicz I., Joly J-P., Rogalska E. (2004). *Langmuir* 20:6259
[22] Torrent-Burgués J., Pla M., Escriche L., Casabó J., Errachid A., Sanz F., J. (2006). *Colloid Interface Sci* 301:585
[23] Xiao X., Liu G., Charych D.H., Salmeron M. (1995). *Langmuir* 11:1600
[24] Woodward J.T., Schwartz D.K. (1996). *J. Am. Chem. Soc.* 118(33):7861
[25] Dufrêne Y.F., Lee G.U. (2000). *BBA-Biomembranes* 1509:14
[26] Leggett G.J. (2003). *Anal. Chim. Acta* 479:17
[27] Carpick R.W., Salmeron M. (1997). *Chem. Rev.* 97:1163
[28] Bhushan B., Israelachvili J.N., Landman U. (1995). *Nature* 374:607
[29] Krim J. (2002). *Surf. Sci.* 500:741
[30] Gnecco E., Bennewitz R., Gyalog T., Meyer E. (2001). *J. Phys.-Condensed Matter* 13:R619
[31] Takano H., Kenseth J.R., Wong S.S., O'Brien J.C., Porter M.D. (1999). *Chem. Rev.* 99:2845
[32] Grant L.M., Tiberg F. (2002). *Biophys. J.* 82:1373
[33] Oncins G., Garcia-Manyes S., Sanz F. (2005). *Langmuir* 21:7373
[34] Green C.P., Lioe H., Cleveland J.P., Proksch R., Mulvaney P., Sader J.E. (2004). *Rev. Sci. Instr.* 75(6):1988
[35] Sader J.E. (1995). *Rev. Sci. Instrum.* 66(9):4583
[36] Cleveland J.P., Manne S. (1993). *Rev. Sci. Instrum.* 64(2):403
[37] Hutter J.L., Bechhoefer J. (1993). *Rev. Sci. Instrum.* 64(7):1868
[38] Florin E.L., Rief M., Lehmann H., Ludwig M., Dornmair C., Moy V.T., Gaub H.E. (1995). *Biosens. Bioelectron*. 10:895
[39] Ogletree D.F., Carpick R.W., Salmeron M. (1996). *Rev. Sci. Instrum*. 67(9):3298
[40] Cain R.G., Reitsma M.G., Biggs S., Page N.W. (2001). Rev. Sci. Instrum. 72(8):3304
[41] Carpick R.W., Sasaki D.Y., Burns A.R. (1999). *Tribol. Lett.* 7:79
[42] Gehlert U., Fang J., Knobler C.M. (1998). *J. Phys. Chem.* B 102:2614
[43] Hisada K., Knobler C.M. (2000). *Langmuir* 16:9390
[44] Evenson S.A., Badyal J.P.S., Pearson C., Petty M.C. (1996). *J. Phys. Chem.* 100:11672
[45] Kajiyama T., Oishi Y., Hirose F., Shuto K., Kuri T. (1994). *Langmuir* 10:1297
[46] Leuthe A., Chi L.F., Riegler H. (1994). *Thin Solid Films* 243:351
[47] Garoff S., Deckman H.W., Dunsmuir J.H., Alvarez M.S., Bloch J.M. (1986). *J. de Physique* 47:701
[48] Mori O., Imae T. (1995). *Langmuir* 11:4779
[49] Hartig M., Chi L.F., Liu X.D., Fuchs H. (1998). *Thin Solid Films* 329:262
[50] Oishi Y., Umeda T., Kuramori M., Suehiro K. (2002). *Langmuir* 18:945
[51] Oishi Y., Kasagi T., Kuramori M., Suehiro K. (2000). *Colloids Surf.* A 169:171
[52] Oncins G., Torrent-Burgues J., Sanz F. (2006). *Tribol. Lett.* 21:175
[53] Matsumoto M., Tanaka K-i., Azumi R., Kondo Y., Yoshino N. (2003). *Langmuir* 19:2802
[54] Matsumoto M., Tanaka K-i., Azumi R., Kondo Y., Yoshino N. (2004). *Langmuir* 20:8728
[55] Imae T., Takeshita T., Kato M. (2000). *Langmuir* 16:612
[56] Ekelund K., Sparr E., Engblom J., Wennerström H., Engström S. (1999). *Langmuir* 15:6946
[57] Rey I., Miñones Jr. J., Dynarowicz P., Miñones J., Conde O. (2004). *Langmuir* 20:11414
[58] Sánchez-González J., Cabrerizo-Vilchez M.A., Gálvez-Ruiz M.J. (1998). *Colloid Polym. Sci.* 276:239
[59] Domenech O., Torrent-Burgués J., Merino S., Sanz F., Montero M.T., Hernández-Borrell J. (2005). *Colloids Surf.* B 41:233
[60] Alsina M.A., Mestres C., Valencia G., Antón J.M.G., Reig F. (1988). *Colloids Surf.* 34:151
[61] Nakahara H., Nakamura S., Kawasaki H., Shibata O. (2005). *Colloids Surf.* B 41:285
[62] Hoda K., Nakahara H., Nakamura S., Nagadome S., Sugihara G., Yoshino N., Shibata O. (2006). *Colloids Surf*. B 47:165
[63] Kurnaz M.L., Schwartz D.K. (1996). *J. Phys. Chem.* 100:11113
[64] Broniatowski M., Dynarowicz P. (2006). *Langmuir* 22:2691
[65] Dynarowicz P., Jawien W., Miñones J., Vila N., Varela C., Iribarnegaray E., Conde O. (1995). *Colloids Surf*. A 97:83
[66] Palacin S. (2000). *Adv. Colloids Interf. Sci.* 87:165
[67] Tatewaki Y., Akutagawa T., Nakamura T., Hasegawa H., Mashiko S., Christensen C.A., Becher J. (2006). *Colloids Surf.* A 284-285:631
[68] Nakanishi T., Ariga K., Morita M., Kozai H., Taniguchi N., Murakami H., Sagara T., Nakashima N. (2006). *Colloids Surf.* A 284-285:607
[69] Rochefeuille S., Berjoan R., Seta P., Jimenez C., Desfours J-P. (2003). *Chem. Phys. Lett.* 376:274
[70] Chou T-H., Chang C-H. (2000). *Colloids Surf.* B 17:71
[71] Martín S., Cea P., Pera G., Haro M., López M.C. (2007). *J. Colloid Interface Sci.* 308:239
[72] Haro M., Giner B., Lafuente C., López M.C., Royo F.M., Cea P. (2005). *Langmuir* 21:2796
[73] Lu W., Guo W., Zhou H., He P. (2000). *Langmuir* 16:5137
[74] Viswanath P., Suresh K.A. (2004). Langmuir 20:8149
[75] del Caño T., Aroca R., de Saja J.A., Rodríguez-Mendez M.L. (2003). *Langmuir* 19:3747
[76] Martín S., Cea P., Lafuente C., Royo F.M., López M.C. (2004). *Surf. Sci.* 563:27
[77] Da Cruz F., Armand F., Albouy P-A., Nierlich M., Ruaudel-Teixier A. (1999). *Langmuir* 15:3653
[78] Wojciechowski K., Grigoriev D., Ferdani R., Gokel G.W. (2006). *Langmuir* 22:8409

[79] Peng J.B., Foran G.J., Barnes G.T., Crossley M.J., Gentle I.R. (2000). *Langmuir* 16:607
[80] Cheng Y., Song W., Cheng J., Zhao B. (2007). *J. Colloid Interface Sci* 307:447
[81] Sheu C-W., Lin K-M., Ku I-H., Chang C-H., Lee Y-L., Yang Y-M., Maa J-R. (2002). *Colloids Surf.* A 207:81
[82] Meyer E., Overney R., Lüthi R., Brodbeck D., Howald L., Frommer J., Güntherodt H-J., Wolter O., Fujihira M., Takano H., Gotoh Y. (1992). *Thin Solid Films* 220:132
[83] Zhang P., Lu J., Xue Q., Liu W. (2001). *Langmuir* 17:2143
[84] Dufrêne Y.F., Barger W.R., Green J-B.D., Lee G.U. (1997). *Langmuir* 13:4779
[85] The scripts are available for non-commercial use at <http://mandm.engr.wisc.edu/faculty_pages_carpick/toolbox.htm>
[86] Brukman M.J., Marco G.O., Dunbar T.D., Boardman L.D., Carpick R.W. (2006). *Langmuir* 22:3988
[87] Outka D.A., Stohr J., Rabe J.P., Swalen J.D., Rotermund H.H. (1987). *Phys. Rev. Lett.* 59:1321
[88] Ulman A., Eilers J.E., Tillman N. (1989). *Langmuir* 5:1147
[89] Barrena E., Kopta S., Ogletree D.F., Charych D.H., Salmeron M. (1999). *Phys. Rev. Lett.* 82:2880
[90] Cappella B., Dietler G. (1999). *Surf. Sci. Reports* 34:1
[91] Kim H.I., Graupe M., Oloba O., Koini T., Imaduddin S., Lee T.R., Perry S.S. (1999). *Langmuir* 15:3179

About the authors

Juan Torrent-Burgués *(Lleida, 1958) graduated in chemistry in 1983 and obtained his PhD in 1988, at the* Universitat de Barcelona (UB). *He is Professor and teaches chemistry, optical materials and coatings, and nanotechnology in the Department of Chemical Engineering of the* Universitat Politècnica de Catalunya (UPC). *Visiting investigator at the University of Utrecht (1990) and at the Centre for Bioelectronics and Nanobioscience (CBEN) at the* Parc Científic de Barcelona *(2003-04), his research fields are electrochemistry, interphases, materials and organized thin films, such as Langmuir and Langmuir-Blodgett films, and their nanomechanical or redox properties. He is member of the Centre of Research in Nanoengineering (CRNE) of the UPC.*

Gerard Oncins *(Lleida, 1979) received a Bsc in Chemistry from the* Universitat de Barcelona *in 2001 and he recently obtained a doctoral degree for his PhD project "Nanomechanics of Organic Layers and Biomembranes" in the Bioelectrochemistry and Nanotechnology research group led by Fausto Sanz (*Universitat de Barcelona *and IBEC). His research is focused on the nanomechanical properties of engineering coatings for MEMS and NEMS as alkanethiols and alkanesilanes, mainly using AFM-based techniques such as Lateral Force Microscopy, Force Spectroscopy and Scanning Polarization Force Microscopy and collaborating in projects with prof. R.W. Carpick (Penn State University) and M. Salmeron (Lawrence Berkeley Laboratory).*

Fausto Sanz *(Barcelona, 1948) graduated in chemistry in 1971 from the* Universitat de Barcelona (UB), *and obtained his PhD in 1975 from the same university. He is a Full Professor and currently teaches in the Department of Physical Chemistry, UB, in the fields of surface science, electrochemistry and SPM applications. Visiting investigator at the University of Utrecht (The Netherlands) (1985-86) and Visiting Scholar at the Lawrence Berkeley Laboratory (University of California at Berkeley) (1991-92), his research started in electrochemistry and progressively developed to include surface science using nanoprobes. He is currently involved in biointerphase projects, having joined the Institute for Bioengineering of Catalunya (IBEC). He is an active member of the Northern California Chapter of the AVS and of the Electrochemical Society.*